Jurnal Kejuruteraan 36(5) 2024: 1795–1803
https://doi.org/10.17576/jkukm-2024-36(5)-01

The Effects of Plate Stiffeners on the Ultimate Load of Square Concrete-Filled Double-Skin Tubular (CFDST) Short Column

Chang Zheng Hao, Mohd Reza Azmi*, Mohd Yazmil Md. Yatim & Ong Tze Sean

Department of Civil Engineering, Faculty of Engineering & Built Environment,
Universiti Kebangsaan Malaysia,
43600 UKM Bangi, Malaysia

**Corresponding author: mohdreza@ukm.edu.my*

Received 2 January 2024, Received in revised form 28 April 2024
Accepted 28 May 2024, Available online 30 September 2024

ABSTRACT

This paper studies the effects of plate stiffeners on the ultimate load of square concrete-filled double-skin tubular (CFDST) short columns under axial compression. The study determines and compares the load-bearing capacity of concrete-filled steel tubular (CFST) short column, CFDST short column and CFDST short columns with plate stiffeners. To achieve these objectives, the researchers performed experimental tests on six composite column specimens: one CFST short column, one CFDST short column and four CFDST short columns with plate stiffeners. The stiffeners are welded to the inner surface of the external tube through pre-drilled holes systematically spaced at four spacings of 10t, 20t, 30t, and 40t, with t represents the external tube thickness. The test results show that the internal steel tubes increased the ultimate strength of the CFDST short columns by approximately 11% compared with the CFST short columns. The CFDST short column with plate stiffeners showed a significant strength improvement of 33% - 42% relative to the CFDST short column. The ultimate strength of CFDST short columns with plate stiffeners increased with smaller intermittent weld spacing of plate stiffeners. Finally, this study proposes a design model that can accurately predict the ultimate strength of CFDST short columns with plate stiffeners with a predicted to experimental strength ratio of 1.02.

Keywords: Concrete-filled double-skin tubular column; internal stiffener; intermittent welding spacing; axial compression; deformation.

INTRODUCTION

Steel-concrete composite structures are extensively used in the present-day construction industry. The present construction method utilises composite to strengthen and reduce construction costs. It is possible to fabricate strong composite columns by incorporating a steel component into concrete columns. The most common composite columns are concrete-filled steel tubular (CFST) columns and concrete-filled double skin tubular (CFDST) columns. The main difference between the two columns is that CFST columns have only one steel tube filled with concrete, while CFDST columns have two steel tubes with concrete poured between them. Compared to the CFST columns, CFDST columns have more advantages, including lower weight because of their hollow centre. The hollow column core reduces the amount of materials required to fabricate the columns. This study focuses on CFDST short columns.

Concerning the strength of the two types of composite columns, the fundamental difference is that the higher strength of the CFDST short columns allows them to bear higher loads; they also have lower self-weight of the internal steel tubes (Yan & Zhao 2020). The study by Ahmed et al. (2020) demonstrated that both steel tube components provide strong support to the concrete, thus enabling it to accommodate all types of loads, including eccentric loads. Compared to circular columns, rectangular columns are generally more susceptible to local buckling. The frequent utilisation of the rectangular shape is because of its simple design and easy production of beam-to-column connections. However, other shapes, such as elliptical, rounded rectangles, hexagons, and dodecagonal, can be used for aesthetic purposes.

Li et al. (2020) investigated the behaviour of sandwich concrete in CFDST short columns and observed some minor cracks in the sandwich concrete. The failure was due to the deflection on both steel tubes. The concrete is assumed to crack gradually and crush during the shear failure. The stability of the column can be improved by incorporating longitudinal stiffeners. The stiffeners along the steel tube slow down the buckling of the steel tube (Huang et al. 2020; Peng et al. 2018; Yuan et al. 2019). There are two welding techniques for constructing stiffened CFST or CFDST short columns using square tubes.: lip-shaped fabrication and plate-by-plate fabrication, as shown in Figure 1 (Wang et al. 2020). However, these welding methods are time-consuming and require the use of steel plates. Therefore, this study employed novel intermittent welding because it eases the fabrication of the stiffened columns and saves time (Chang et al. 2022). For these reasons, designers, infrastructure operators and researchers continue to show great interest in the behaviour of CFDST short columns with plate stiffeners.

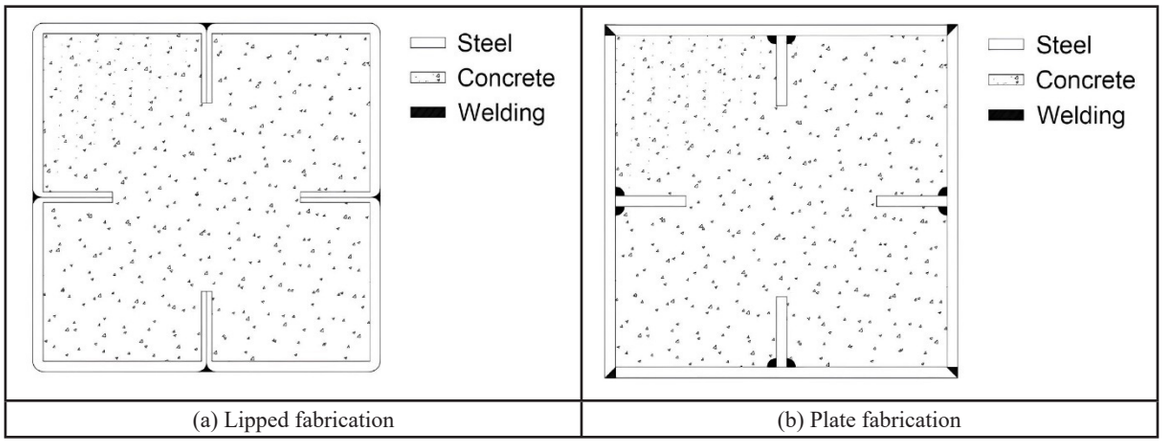

FIGURE 1. Plate stiffened CFST short column

This study aims to create a cost-effective and efficient design formula for estimating the ultimate load of plate stiffened CFDST short columns, as an alternative to full-scale testing. However, the current ACI-318 (2014) code falls short in designing CFDST short columns with intermittently welded plate stiffeners, providing overly conservative results due to inadequate consideration of confined concrete and the confinement effect of the plate stiffeners, as noted by Hassanein et al. (2013). Thomas & Sandeep (2020) reported the experimental results for 29 CFST short columns with intermittent welded plate stiffeners. They proposed a set of formulas for calculating the ultimate load using the von Mises yield criterion to depict the forces acting on the internal concrete of the CFST short columns by the external steel tube. The formulas were based on Ho and Lai (2013), who introduced intermittent welding on the circular CFST short column with tension rods that consider the effect of confining pressure on the core concrete. Hassanein and Kharoob (2014) conducted a review of various design models to formulate estimates for the ultimate load of CFDST short columns based on the external tube's diameter-to-thickness ratio. The experimental test in this research was carried out on CFDST with intermittently welded plate stiffeners. The investigated parameters are the effect of the internal steel tube in CFST compared to CFDST, the effects of plate stiffeners on the CFDST short column and the intermittent weld spacing. The study also introduced a design model formulated from the experimental findings.

DETAILS OF TESTS

The study involved subjecting four CFDST short columns with plate stiffeners, one CFDST short column, and one CFST short column to axial compression to assess their load-bearing capacity and examine their failure behaviour at the ultimate load. All plate stiffeners are continuous in the longitudinal direction and have the same height as the CFDST short columns (360 mm). The external steel tube has a dimension of 100 mm × 100 mm and a 2.3 mm steel thickness. The internal steel is 32 mm × 32 mm and has a 2.0 mm steel thickness. The diameter of the intermittent weld holes, l_w, is 6 mm. The cross-sectional and overall views of the specimens, along with their typical geometry and notations, are depicted in Figure 2. B_o and D_o are the external steel breadth and width, respectively; t_o is the external steel thickness; B_i and D_i are the internal steel

breadth and width, respectively; and t_i is the internal steel thickness. b_s is the plate stiffener width, and t_s is the plate stiffener thickness.

The letter S in the specimen designation represents the square cross-section. The diameter of the external and internal steel tubes remained constant at 100 mm and 32 mm throughout the test. The plate stiffener has a dimension of 18*a* (18 mm × 2.3 mm). The spacing between the welds was determined as 10*t*, 20*t*, 30*t*, and 40*t*, where *t* is the external tube thickness as suggested by Thomas & Sandeep (2020). Table 1 provides geometry details of the specimens.

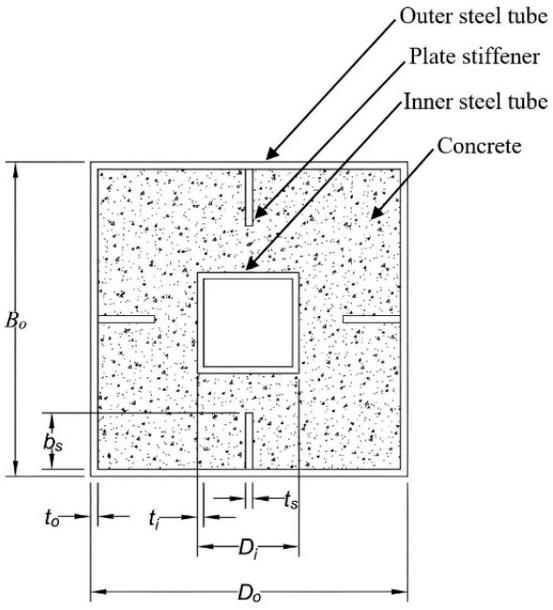

(a) Cross-sectional area

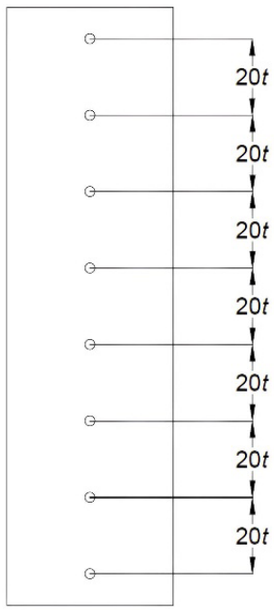

(b) 3D view

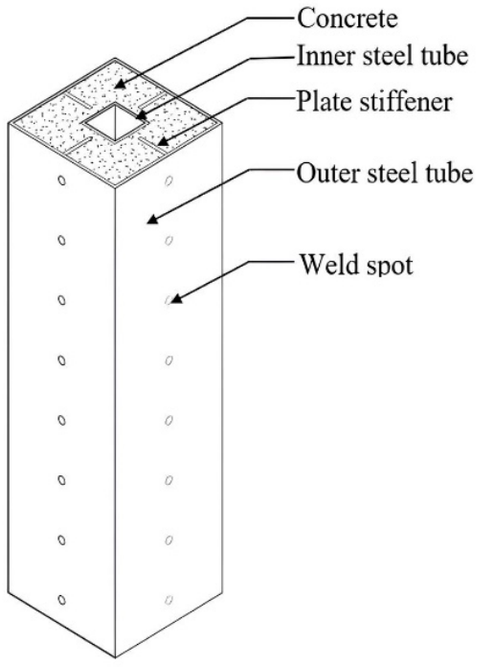

(c) Weld spacing

FIGURE 2. Typical details of the plate stiffened CFDST short column

TABLE 1. Specimen Geometry

Specimen	Inner tube		Stiffener		Weld spacing (mm)	Weld spacing from end (mm)	No. of weld holes (one side)
	B_o (mm)	t_i (mm)	b_s (mm)	t_s (mm)			
S100	-	-	-	-	-	-	-
S100/32	32	2.0	-	-	-	-	-
S100/32-18*a*-10*t*	32	2.0	18	2.3	23	19	15
S100/32-18*a*-20*t*	32	2.0	18	2.3	46	19	8
S100/32-18*a*-30*t*	32	2.0	18	2.3	69	7.5	6
S100/32-18*a*-40*t*	32	2.0	18	2.3	92	42	4

SPECIMENS AND TEST EQUIPMENT

The design of the test specimens was patterned after those examined by Thomas & Sandeep (2020) and customized to meet the objectives of this study. Steel coupons were cut from the steel tube, adhering to the shape and dimensions outlined in ASTM A370 (2014). Table 2 provides the mean values for Young's modulus $E_{(avg)}$, yield stress $f_{y\,(avg)}$ at 0.2% plastic strain, and ultimate stress $f_{u\,(avg)}$. The concrete-to-cement mix ratio is 1.00: 0.54: 2.23: 1.49 (cement: water: fine aggregate: coarse aggregate). Cube tests with dimensions of 150 mm × 150 mm × 150 mm were conducted, resulting in an average concrete cube strength (f_{cu}) of 31.9 MPa.

TABLE 2. Steel properties

Coupon	Yield stress $f_{y\,(avg)}$ (MPa)	Ultimate stress $f_{u\,(avg)}$ (MPa)	Young's modulus $E_{(avg)}$ (GPa)
Outer steel	268.3	389.9	209.1
Inner steel	265.1	378.8	208.8
Plate stiffener	258.5	373.2	206.3

Figure 3 shows the pre-drilled intermittent weld holes. The plate stiffener is aligned properly to the pre-drilled weld holes in the external tube and the welding is performed from the outside. A weld inspection is carried out after the welding has been completed. The final step is sanding the welded holes to ensure there is no irregularity or poor welding. The external and internal hollow steel tubes are welded onto the end plate to make sure the hollow steel tubes remain aligned throughout the casting. The hollow area of the internal steel tube is covered with a plastic film to prevent concrete from accidentally entering the hollow core. The concrete is then mixed and poured into the spaces between the external and internal steel tubes.

Figure 4 illustrates a standard specimen loading arrangement. The experiment is carried out utilizing a compression machine with a 2000-kN capacity. On the top loading plate, two LVDT transducers are positioned to measure the vertical displacement throughout the tests. Real-time displacement data of the specimens are recorded by these LVDT transducers, which are linked to a local computer through data logger software. The specimens undergo concentric loading with a progressively increasing rate of 5 kN/s.

FIGURE 3. Typical pre-drilled intermittent weld holes

FIGURE 4. Typical specimen loading setup

RESULTS AND DISCUSSION

ULTIMATE LOAD CAPACITY

The test findings indicate that the composite column's ultimate load is increased with the addition of the internal steel tube. The control specimen S100 is a CFST short column without an internal steel tube. The CFDST short column S100/32 exhibited an 11% improvement in ultimate strength compared to the CFST short column. The steel tubes, both external and internal, act as a cover that confines the internal concrete from expanding. The higher steel ratio of the column also increases its ability to endure additional loading. The plate stiffened CFDST short columns exhibit an ultimate load that is 33 - 44% more than that of the unstiffened CFDST short column. These results show that the plate stiffeners increase column ultimate strength by providing extra longitudinal support when loaded under axial compression. The plate stiffeners can carry a higher axial loading and thus provide additional confinement to the internal concrete. Moreover, the composite action of these materials is enhanced due to the increase in contact surface between the concrete and the steel.

The plate stiffeners were intermittently welded onto the CFDST short columns. The ultimate strength decreased markedly with higher intermittent weld spacings. For instance, the ultimate strength of specimen S100/32-18*a*-10*t* is 6% higher than specimen S100/32-18*a*-40*t*. The number of weld holes decreases with larger intermittent weld spacing, resulting in the plate stiffeners not being firmly attached to the external steel tube and more movement of the plate stiffeners in the CFDST short column when loaded axially. The experimental result underscores the advantage of utilising intermittent welded plate stiffeners as stiffening element in the CFDST short column. Table 3 summarises the variations in the ultimate load, P_u, of all specimens.

TABLE 3. Experimental result

Specimen	Ultimate Load, P_u *(kN)*
S100	534
S100/32	592
S100/32-18*a*-10*t*	841
S100/32-18*a*-20*t*	832
S100/32-18*a*-30*t*	816
S100/32-18*a*-40*t*	789

LOAD-DISPLACEMENT BEHAVIOUR

The load-displacement curves illustrated in Figure 5 showcase how intermittent welded plate stiffeners influence the overall behaviour of the CFDST short column. The CFDST short column, when equipped with plate stiffeners,

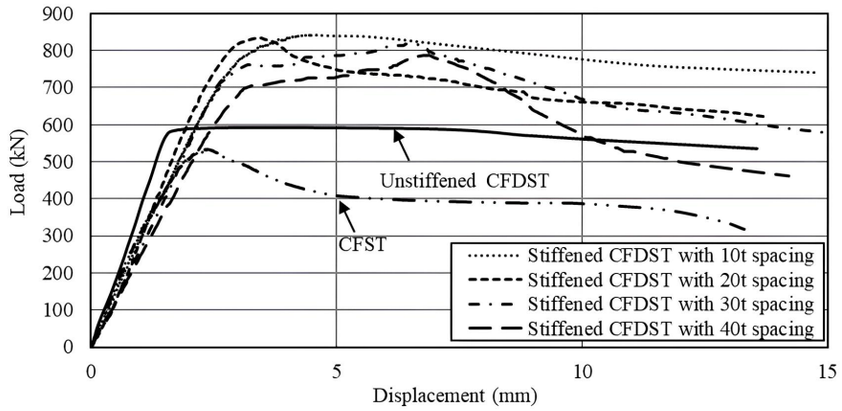

FIGURE 5. The relationship between the load-displacement responses of each stiffened CFDST with the control specimens

has a superior ultimate load capacity compared to both the unstiffened CFDST and CFST short columns. The curves for all columns are linear before reaching the ultimate load; they gradually lose their strength post the ultimate load and can no longer sustain the axial compression. Upon reaching the ultimate strength capacity, the concrete cracked and the majority of the residual strength is transferred to the steel tubes around it. As a result, the vertical force applied to the column begins to decrease.

FAILURE CHARACTERISTICS

The test specimens were loaded gradually with a uniform rate. In the initial phase, the column shows a linear elastic behaviour, and the deformation was negligible. The double steel tubes and the plate stiffeners enclosing the sandwich concrete give it better elastic behaviour and concentrate the forces primarily within the concrete. As the load increases, the concrete gradually expands until it detaches from the steel components, and the load bearing forces begin to shift towards the steel components. The deformation of the columns becomes apparent as the column approaches its ultimate strength, and the outward buckling is visible as forces act on the external steel tubes.

In all cases, the test specimens undergo outward local buckling. The black circle indicating the buckling deformation in Figure 6 is a local buckling. Figure 6(a)-(c) shows that the specimens experience elephant foot buckling because of the lack of additional stiffeners at the tip of the column. Figures 6(d) and 6(e) show the columns undergoing local buckling at quarter height, and Figure 6(f) shows the column experiencing two outward bucklings. These bucklings are due to the crushed internal concrete expanding and deforming the external steel tube.

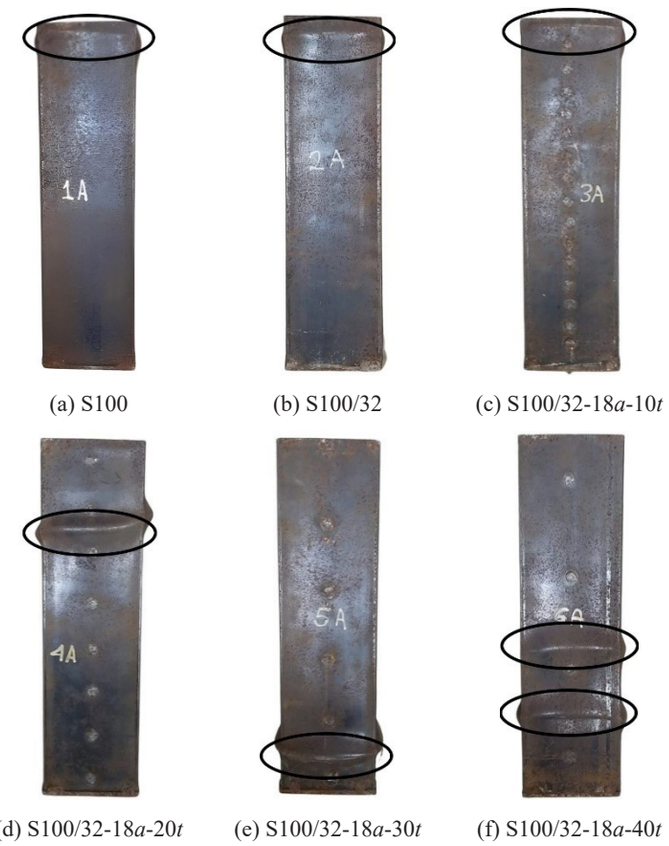

(a) S100 (b) S100/32 (c) S100/32-18*a*-10*t*

(d) S100/32-18*a*-20*t* (e) S100/32-18*a*-30*t* (f) S100/32-18*a*-40*t*

FIGURE 6. The deformation shapes of the test specimens

DESIGN OF THE PLATE STIFFENED CFDST SHORT COLUMN

Equation (1) is employed for determining the ultimate load on CFDST short columns with intermittently welded plate stiffeners. This equation involves the cumulative sum of loads carried by various components, such as external and internal steel tubes, confined concrete, and plate stiffeners. Factors like intermittent weld spacing and the height of the column specimens are taken into account in the design

equation. The estimation of uni-axial stress in the steel tube is based on the Von-Mises yield criterion (Ho & Lai 2013), as outlined in Equation (2).

$$P_{u,p} = A_s\sigma_{sz} + A_{si}f_{yi} + A_cf_{cc} + A_{st}f_{st} \quad (1)$$

$$\sigma_{s\theta}^2 + \sigma_{s\theta}\sigma_{sz} + \sigma_{sz}^2 = \sigma_{sy}^2 \quad (2)$$

$$\frac{\sigma_{s\theta}}{\sigma_{sy}} = 0.046\xi + 0.174\ for\ (1/9 \le \xi \le 5.3) \quad (3)$$

$$\xi = A_s\sigma_{sy}/A_cf'_c \quad (4)$$

The cross-sectional area of the external steel tube is represented by A_s, A_{si} is the cross-sectional area of the internal steel tube, A_c is the cross-sectional area of the concrete, and A_{st} is the cross-sectional area of the plate stiffeners. The symbols σ_{sz},f_{yi},f_{cc}, and f_{st} denote the uni-axial failure stress of the external steel tube, yield strength of the internal steel tube, strength of the confined concrete, and yield strength of the plate stiffeners, respectively. Under the Von-Mises criterion, $\sigma_{s\theta}$ represents the hoop stress in the steel tube, σ_{sy} is the uni-axial yield strength of steel (also known as f_y), and ξ denotes the confinement index.

The calculation of f_{cc} employs the method proposed by Cusson & Paultre (1994). Since the study uses a compressive strength, $f_{cu,}$ of 150 mm cube test, the f_{cu} is converted to an equivalent cylinder strength, f'_c, using the equation by L'Hermite (Mirza & Lacroix 2004). k_p is the confinement efficiency factor suggested by Thomas & Sandeep (2020), f_r denotes the pressure exerted by the steel tube on the inner concrete, n is the amount of plate stiffeners, l_w signifies the weld hole diameter, and s is the intermittent weld spacing. B_o represents the external steel tube width, B_i is the internal steel tube width, and t_o is the thickness of the external steel tube. H indicates the specimen height, b_s represent the plate stiffener width, and t_s represent the plate stiffener thickness.

$$f_{cc} = f_c' + k_pf_r \quad (5)$$

$$f'_c = [0.76 + 0.2\log_{10}\left(\frac{f_{cu}}{19.6}\right)]f_{cu} \quad (6)$$

$$k_p = 2.368\left(\frac{nl_w}{1+s}\right) + 4.1 \quad (7)$$

$$f_r(B_o - 2t_o - B_i)H = 2\sigma_{s\theta}tH + nf_{st}b_st_s \quad (8)$$

Figure 7 illustrates the confining pressure f_r in terms of the geometry and hoop stress of the steel tube by considering the free body diagram. The ultimate loads reported were compared with predicted loads in Table 4. The average predicted to experimental strength ratio is 1.02, indicating a strong correlation between the experimental data and the predictions based on the proposed method.

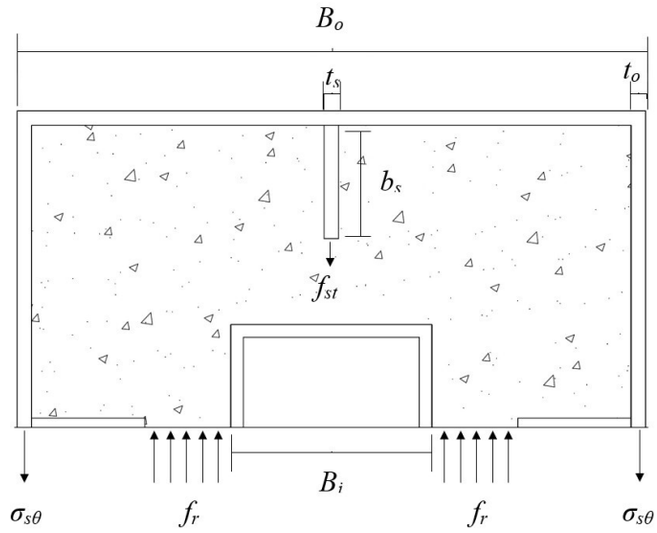

FIGURE 7. Free body diagram for confining stress (with plate stiffeners)

TABLE 4. Comparison of the experimental result with the design model

Specimen	Ultimate Load, P_u *(kN)*	Predicted Load, $P_{u,p}$ (kN)	$P_u / P_{u,p}$
S100	534	550	0.97
S100/32	592	626	0.95
S100/32-18*a*-10*t*	841	842	1.00
S100/32-18*a*-20*t*	832	784	1.06
S100/32-18*a*-30*t*	816	764	1.07
S100/32-18*a*-40*t*	789	754	1.05
Average			1.02

CONCLUSION

This research conducted an axial compression experiment involving six composite short columns. These columns comprised four CFDST short columns with plate stiffeners, one CFDST short column, and one CFST short column. The key result of the fundamental research is that the ultimate load of the plate stiffened CFDST short column increased by 33% - 42% compared to the unstiffened CFDST short column. The experimental data revealed variations in ultimate strength based on different intermittent weld spacings, with specimens having closer weld spacing exhibiting a higher ultimate load capacity. These findings highlight that the incorporation of longitudinal internal plate stiffeners significantly enhance the ultimate load of CFDST short columns. The study introduces a design model aimed to estimate maximum capacity of plate stiffened CFDST short columns. Additionally, the research provides comprehensive insights into the ultimate load and the behaviour of CFDST short columns with intermittently welded plate stiffeners.

ACKNOWLEDGEMENT

The authors acknowledge the Fundamental Research Grant Scheme (FRGS). Grant number FRGS/1/2020/TK0/UKM/03/6 funded by the Ministry of Higher Education (MOHE), Malaysia and the facilities provided by the Department of Civil Engineering, Universiti Kebangsaan Malaysia.

DECLARATION OF COMPETING INTEREST

None.

REFERENCES

ACI-318. 2014. *Building Code Requirements for Structural Concrete*. American Concrete Institute.

Ahmed, M., Liang, Q.Q.Q., Patel, V.I., Hadi, M.N.S.,

Steel, M.H.-J. of C. & 2020, U. 2020. Experimental and numerical investigations of eccentrically loaded rectangular concrete-filled double steel tubular columns. *Journal of Constructional Steel Research 167*(May): 105949. https://www.researchgate.net/publication/341756889.

ASTM A370. 2014. A370: Standard Test Methods and Definitions for Mechanical Testing of Steel Products.*ASTM International* 1–50.

Chang, Z.H., Azmi, M.R. & Md. Yatim, M.Y. 2022.

Behaviour of Concrete-Filled Double Skin Tubular Short Column with Plate Stiffeners Welded Intermittently under Axial Compression. *Buildings 12*(5): 567. https://www.mdpi.com/2075-5309/12/5/567.

Cusson, D. & Paultre, P. 1994. High-Strength Concrete Columns Confined by Rectangular Ties. *Journal of Structural Engineering 120*(3): 783–804. https://ascelibrary.org/doi/10.1061/%28ASCE%290733-9445%281994%29120%3A3%28783%29.

Hassanein, M.F. & Kharoob, O.F. 2014. Compressive strength of circular concrete-filled double skin tubular short columns. *Thin-Walled Structures 77*: 165–173. http://dx.doi.org/10.1016/j.tws.2013.10.004.

Hassanein, M.F., Kharoob, O.F. & Liang, Q.Q. 2013. Circular concrete-filled double skin tubular short columns with external stainless steel tubes under axial compression. *Thin-Walled Structures 73*: 252–263. https://doi.org/10.1016/j.tws.2013.08.017.

Ho, J.C.M. & Lai, M.H. 2013. Behaviour of uni-axially loaded CFST short columns confined by tie bars. *Journal of Constructional Steel Research 83*: 37–50. https://doi.org/10.1016/j.jcsr.2012.12.014.

Huang, L., Zhang, S.S., Yu, T. & Peng, K.D. 2020. Circular hybrid double-skin tubular columns with a stiffener-reinforced steel inner tube and a large-rupture-strain FRP outer tube: Compressive behavior. *Thin-Walled Structures 155*. https://doi.org/10.1016/j.tws.2020.106946

Li, W., Chen, B., Han, L.H. & Lam, D. 2020. Experimental study on the performance of steel-concrete interfaces in circular concrete-filled double skin steel tube. *Thin-Walled Structures 149*. https://www.sciencedirect.com/science/article/pii/S0263823119318191.

Mirza, S.A. & Lacroix, E.A. 2004. Comparative Strength Analyses of Concrete-Encased Steel Composite Columns. *Journal of Structural Engineering 130*(12): 1941–1953. https://doi.org/10.1061/(ASCE)0733-9445(2004)130:12(1941).

Peng, K., Yu, T., Hadi, M.N.S. & Huang, L. 2018. Compressive behavior of hybrid double-skin tubular columns with a rib-stiffened steel inner tube. *Composite Structures 204*: 634–644. https://doi.org/10.1016/j.compstruct.2018.07.083.

Thomas, J. & Sandeep, T.N. 2020. Capacity of short circular CFST short columns with inner vertical plates welded intermittently. *Journal of Constructional Steel Research 165*: 105840. https://doi.org/10.1016/j.jcsr.2019.105840.

Wang, Z.B., Zhang, J. Bin, Li, W. & Wu, H.J. 2020. Seismic performance of stiffened concrete-filled double skin steel tubes. *Journal of Constructional Steel Research 169*: 106020. https://www.sciencedirect.com/science/article/pii/S0143974X19312246.

Yan, X.F. & Zhao, Y.G. 2020. Compressive strength of axially loaded circular concrete-filled double-skin steel tubular short columns. *Journal of Constructional Steel Research 170*: 106114. https://www.sciencedirect.com/science/article/pii/S0143974X1931291X.

Yuan, F., Huang, H. & Chen, M. 2019. Effect of stiffeners on the eccentric compression behaviour of square concrete-filled steel tubular columns. *Thin-Walled Structures 135*(11): 196–209. https://doi.org/10.1016/j.tws.2018.11.015.